Multi-domain analysis of microvascular flow motion dynamics

Andrew J Chipperfield[1], Marjola Thanaj[1], Eleonora Scorletti[2], Christopher D Byrne[2] and Geraldine F Clough[2]

[1]Faculty of Engineering and Physical Sciences and [2]Faculty of Medicine, University of Southampton, UK

Key words: microcirculation, blood flow, flow motion, frequency analysis, complexity

Short title: Microvascular flow motion dynamics

Address for Correspondence:

Andrew Chipperfield BSc PhD

Bioengineering Science

School of Engineering

Faculty of Engineering and Physical Sciences

University of Southampton

Highfield

Southampton SO17 1BJ. UK

Email: a.j.chipperfield@soton.ac.uk

Telephone: (0)23 8059 8344

Abstract

Objective: To determine whether analysis of microvascular network perfusion using complexity-based methods can discriminate between groups of individuals at an increased risk of developing CVD.

Methods: Data were obtained from laser Doppler recordings of skin blood flux at the forearm in 50 participants with non-alcoholic fatty liver disease grouped for absence (n=28) or presence (n=14) of type 2 diabetes and use of calcium channel blocker medication (n=8). Power spectral density was evaluated and Lempel-Ziv complexity determined to quantify signal information content at single and multiple time-scales to account for the different processes modulating network perfusion.

Results: Complexity was associated with dilatory capacity and respiration and negatively with baseline blood flux and cardiac band power. The relationship between the modulators of flowmotion and complexity of blood flux is shown to change with time-scale improving discrimination between groups. Multiscale Lempel-Ziv achieved best classification accuracy of 86.1%.

Conclusions: Time and frequency domain measures alone are insufficient to discriminate between groups. As CVD risk increases, the degree of complexity of the blood flux signal reduces, indicative of a reduced temporal activity and heterogeneous distribution of blood flow within the microvascular network sampled. Complexity-based methods, particularly multiscale variants, are shown to have good discriminatory capabilities.

Key words: microcirculation, blood flow, flow motion, frequency analysis, complexity

Abbreviations

BF, blood flux

CVD, cardiovascular disease

FFT, fast Fourier transform

LDF, laser Doppler fluximetry

LF, low frequency

HF, high frequency

LZC, Lempel and Ziv complexity

LDA, linear discriminant analysis

Met, metabolic

MLZC, multiscale Lempel and Ziv Complexity

NAFLD, non-alcoholic fatty liver disease

PORH, post occlusive reactive hyperaemia

PSD, power spectral density

T2DM, type 2 diabetes mellitus

1. Introduction

An adequate delivery of blood flow through a vascular network, commensurate with the metabolic demands of the tissue, is reliant on regulation of microvascular perfusion, predominately achieved through changes in network conductance and modulated at a local level by endothelial, neurogenic and myogenic regulatory activity[1]. It has been argued that attenuation or alteration of these flow regulatory mechanisms may be a major contributor to disease risk and that quantitative measures of temporal behavior and spatial distribution of microvascular perfusion, in vivo, are imperative if we are to understand how variation in functionality and flexibility occur in cardiovascular (CV) and metabolic (Met) disease[2,3].

Non-invasive assessment of skin microvascular blood flow has been used widely to evaluate microvascular impairment and CVD risk factors on vascular health in both research and clinical practice[4]. To date, time and frequency domain analysis of signals obtained using Laser Doppler flowmetry (LDF) in superficial vascular networks such as that of the skin has been extensively used to describe the dynamic and non-linear characteristics of flow patterns. Spectral analysis of the frequency components of the LDF signal have been shown to reflect the influence of endothelial (0.0095-0.02 Hz) and sympathetic (0.02-0.06 Hz) activity, myogenic activity in the vessel wall (0.06-0.15 Hz), respiration (0.15- 0.4 Hz) and heart beat (0.4-1.6 Hz) on local tissue perfusion[5]. Variations in the amplitude and relative contribution of the spontaneous, rhythmic oscillatory fluctuations of both local (endothelial, neurogenic, and myogenic) and systemic origin have been associated with a decline in microvascular function in individuals at risk of, or with CV and Met disease[6]. However, time and frequency domain analysis have not proved sufficient for the classification of tissue perfusion features in different pathophysiological groups or provided consistent interpretation of microvascular function.

More recently, the regularity and the randomness of the microvascular network perfusion has been explored using non-linear methods such as entropy and complexity techniques, respectively. Studies in a primate model of diabetes have shown a reduced complexity of the blood flux (BF) signal using a Lempel-Ziv complexity (LZC) algorithm[7], while in humans with a familial predisposition to hypertension, altered microvascular haemodynamic have been associated with diminished chaotic ischaemic flow[8]. In rodent models of CV and Met disease, chaotic network attractor analysis has revealed a declining adaptability of microvascular flow patterns[9]. Thus it might be expected that an altered spatial heterogeneity and temporal stability of network perfusion will limit the adaptive

capability of the microvasculature to meet changing metabolic needs. We have previously shown this to be the case using combined LDF and white light spectroscopy to measure microvascular blood flow and tissue oxygenation[10,11]. These more recent studies suggest that nonlinear measures may be of benefit in investigating the dynamics within the microcirculation to discriminate more effectively between different influences on network functionality and flexibility.

The primary objective of this study was to examine and compare the time, frequency and complexity of the oscillatory rhythms in microvascular blood flow in a group of people with non-alcoholic fatty liver disease (NAFLD) at risk of cardiovascular disease (CVD). A further aim was to improve understanding of the relationship between assessment metrics in the different analysis domains and the signal from which they arise. Ultimately, this should lead to better-informed differentiation or categorization of measured BF signals. Data sets were obtained from volunteers with and without type 2 diabetes mellitus (T2DM) and a smaller group using calcium channel blockers. The purpose was to test the hypothesis that complexity-based methods used to analyze the BF in microvascular network could discriminate between the different groups. Absolute flow and a vasoprovocation test were examined in the time domain and the spectral content of the LDF signal examined in the frequency domain. The complexity, or information content, was then assessed and, to examine if this was influenced by the time-scale of the different oscillatory rhythms, a multiscale complexity method evaluated.

2. Materials and Methods

Ethical Approval

The study was approved by the Research Ethics Committee of the University of Southampton and Southampton General Hospital (REC: 08/H0502/165). The study was performed in accordance with standards set by the Declaration of Helsinki. All participants gave written informed consent.

Study Design

Fifty volunteers with NAFLD[12] (30 men; 20 women) age 52.6 ± 6.8 years and BMI 33.0 ± 5.2 kg/m^2 (mean $\pm$ SD) participated in this study. They were grouped for the absence (DM0) or presence (DM1) of T2DM, and use of calcium channel blocker medication (CB) with and without T2DM (5 with T2DM). Composition and parameters of the three groups are given in Table 1. All participants refrained from caffeine containing drinks and food for at least 2 hours and strenuous exercise for 24 hours before testing.

Studies were performed in a temperature-controlled room maintained between 22 and 23.5°C. All participants were acclimatized for 30 minutes prior to testing. The mean resting forearm skin temperature measured during baseline recording was 29.4 ± 2.1°C. Laser Doppler measurements were made with the participants sitting comfortably with their arm supported at heart level. Data supporting this study are openly available from the University of Southampton repository at https://doi.org/10.5258/SOTON/D0781

LDF Signal Capture

Skin BF and temperature were measured by laser Doppler fluximetry (VMS LDF, Moor Instruments Ltd, UK) using a 785 nm, 1 mW low power red laser light source with fiber separation of 0.5 mm and integral thermistor sensor (VP1-V2, Moor Instruments Ltd, UK) according to the manufacturers safety requirements. Calibration of the probes was performed using aqueous suspension of polystyrene latex particles whose Brownian motion provides a standard reference value. The probe was mounted using double sided sticky O-rings on the ventral surface of the non-dominant forearm, approximately 10cm from the wrist avoiding visible veins. Signals were recorded at a sampling rate of 40 Hz.

Baseline skin BF and temperature were recorded for 15 minutes before manipulation of tissue perfusion by reactive hyperaemia to transient arterial occlusion using a pressure cuff placed around the upper arm inflated to 180 mmHg for three minutes (PORH). We have previously shown that the inter-individual coefficient of variation (CV) for resting BF in a cohort of 10 healthy individuals at ambient room temperature was 0.15[13] (CV values < 0.35 taken as acceptable[14]). The inter-class correlation coefficient (ICC) for resting BF (n = 10) was 0.85 (almost perfect[15]).

Signal Analysis

Time-domain: BF was recorded in arbitrary perfusion units (PU). Values for BF parameters were determined using moorVMS-PC software (Moor Instruments Ltd, UK) at baseline over the final 5 min before perturbation of BF (RF); the 3 min arterial occlusion (value taken as equivalent to Biological Zero); peak reactive hyperaemia (MF). All signal segments were checked to be clear of artefacts.

Frequency-domain: Prior to spectral analysis, 10 min segments of artefact free baseline BF signals were filtered using a finite impulse response low-pass filter with 2 Hz cut-off to attenuate high frequencies beyond the known range of microvascular oscillation. The data segments were then

detrended by removing the mean. Spectral density was estimated by Welch's method of fast Fourier transform (FFT) with a Hanning window size of 200 s and 50% overlap between windows over continuous 10 min recording periods using MATLAB (R2018a, MathWorks, UK). The power contribution was evaluated within the frequency range (0.0095-1.6 Hz), divided into frequency intervals corresponding to endothelial (0.0095 – 0.02 Hz), sympathetic (0.02 – 0.06 Hz), myogenic (0.06 – 0.15 Hz), respiratory (0.15 – 0.4 Hz) and cardiac (0.4 – 1.6 Hz) activity[16]. Total spectral power was estimated as the sum of absolute power across the five frequency intervals (0.0095-1.6 Hz) and expressed in PU^2/Hz. Power spectral density (PSD) contribution was calculated relative to total spectral power and is expressed as a fraction between 0 and 1.

Complexity: To examine how much baseline BF signals from the test groups differ from a random sequence we calculate the LZC[17] of its binary representation[18]. To reduce any bias from measurement noise or frequency components outside the range of interest, the sme low pass filtering and detrending used in the frequency domain analysis was applied the raw BF signals before calculating their complexity measure. Binary representation of biomedical signals has been reported as suitable for estimating their complexity in previous studies, e.g.[19,20]. LZC has been used to estimate and quantify symbolic sequences converted from a time series[7,20,21] to determine the information present in a signal or sequence. The sequence is parsed from left to right and the complexity increases by one unit when a new sub-sequence of continuous symbols is encountered. The greater the number of sub-sequences, the more information that is present in the data sequence and the higher the complexity, *C*. Here we normalize the complexity to the sequence length, *n*, as $C_{norm} = C/(n/\log_2(n))$.

In previous work[10, 22], we have shown that these LZC measures can be used to discriminate between two haemodynamic steady states (resting and that induced by local thermal hyperaemia) and are thus a good candidate for the study presented here. In Tigno et al[7], using vasomotion to predict metabolic risk groups in nonhuman primates, this sequence is determined by comparing each element in the time series with the median value and replacing it with a zero if it is less than the median or a one otherwise. As suggested by Yang et al[23], we have used a delta encoding method whereby a zero is recorded if a value is less than the previous value in the time series or as a one when it is greater than that previously as this captures more of the dynamics in the signals. Exhaustive LZC is then calculated for each epoch as it gives the lower limit for LZC estimation since the components of a sequence are not reproduced. A LZC-index was calculated as the mean of the 15 × 40 second epochs for each sampled signal.

LZC is used to analyze the BF on a single scale. However, it is known that the BF signal is modulated by at least 5 physiological process, operating at frequencies ranging from 0.001Hz to 2Hz, and these multiple process scales should be taken into account. To test whether the BF signals are consistent over multiple spatial and temporal scales, and do not change with sampling frequency, we also measure LZC in multiple time scales. A coarse-graining approach, introduced by Costa et al[24] in multiscale entropy analysis, resamples the original signal by reducing the scale of the time series. The sampling frequency of the signal is altered by a scale factor τ, which defines the number of sampling levels. So, for a time series $\{x_1,\ldots,x_N\}$, the coarse-grained time series, y^τ, will be:

$$y_i^\tau = \frac{1}{\tau}\sum_{i=(i-1)\tau+1}^{i\tau} x_j \,, 1 \le i \le N/\tau. \quad (1)$$

For a scale factor of one the time series y^1 is the original signal. So, the length of each time series $\{y^\tau\}$ is equal to the length of the original signal divided by the scale factor, τ. At the coarse-grain of 24 scales, the signal length is 1000 which we show in[22] is sufficient for complexity analysis. The LZC was calculated for each coarse-grained sequence as a function of the scale factor, τ, and the multiscale Lempel and Ziv complexity (MLZC) was evaluated.

Statistical Analysis

Statistical analysis was performed using GraphPad Prism (Prism 7, GraphPad Software, Inc., USA) and IBM SPSS Statistics 25 (IBM United Kingdom Limited, UK). Data were tested for normal distribution using D'Agostino & Pearson omnibus normality test and presented as either mean ± standard deviation (SD) for normally distributed data or median with interquartile range (IQR) for non-normally distributed data. Normally distributed data were compared using a Student t-test and non-normally distributed data using a Mann-Whitney test. Pearson or Spearman correlation coefficients are presented for univariate regression analysis of baseline data. In all cases a value of $p < 0.05$ was taken to indicate statistical significance.

Linear discriminant analysis (LDA) with leave-one-out cross-validation[25,26] was applied to complexity measures of BF signals, to determine classification accuracy between groups. The LDA method was applied to transform the features from a higher to a lower dimensional space. For LZC the features are the 15 epochs and for MLZC they are the 24 different scales. In this way the ratio of the distance between the means of the classes in the projected space and the scatter within each class is maximized and thereby the classes are maximally separated. The accuracy was assessed using the

leave-one-out cross-validation in which 30 runs took place, and in each run the classifier trains the set apart from one sample which was presented as the test set[24].

3. Results

There was a significant difference (p<0.05) between BMI of the CB group and the other two groups and between the HbA1c of DM0 and DM1. Blood pressure, measured using a standard sphygmonometer before the test after acclitization, shows hypertension in all groups but no significant difference between them. Homeostatic model assessment of insulin resistance (HOMA-IR)[27] data suggest that most subjects were insulin resistant and subjects in the DM1 and CB group were more insulin resistant than subjects in the group without diabetes. Average daily energy expenditure as assessed by metabolic equivalent of task (METS) and measured by the SenseWear Pro2/3 armband (BodyMedia, PA, USA), indicate a sedentary or inactive lifestyle in most subjects[28]. CVD risk was determined from the QRISK2 calculator[29] and showed that estimated CVD risk was higher in subjects with diabetes than subjects without diabetes.

Time domain

As has extensively been reported in the literature, little useful information can be gleaned from directly examining LDF signals[4,30,31]. Consider the BF signals shown in Figure 1 (A and B) recorded from skin at the forearm of two different people with and without T2DM. The signal in Figure 1 (A) appears to have a lower mean value but more pronounced variation in moving average than that in Figure 1 (B), which also shows larger higher frequency variations. The LDF signal, defined as blood flux, is the product of red blood cell concentration and velocity. The depth of tissue from which it is derived depends on laser power, wavelength and separation of emitting and receiving fibres[32] and can exhibit significant spatial variation[33]. Thus, LDF provides a relative index of microvascular perfusion in the time domain and is frequently used with a vasoreactivity test, such as the PORH shown in Figure 1 (C), to investigate dilator capacity and processes regulating local vascular tone[34].

The resting blood flux (RF), determined as the mean BF over 5 minutes before perturbation, and the fold change MF/RF, determined as the ratio of the mean peak of the PORH divided by RF, are shown in Table 2. The DM0 group has lowest RF and the CB group the lowest dilatory capacity. Significant difference was found in RF between those without T2DM and those taking calcium channel blockers

(p = 0.012) and in dilatory capacity between DM0 and CB (p = 0.017) and DM1 and CB (p = 0.012). Dilator capacity and RF reduced with and calcium channel use. So, while the reactive test can discriminate between groups, it cannot discriminate between them reliably or sufficiently for the groups studied here. As the BF is modulated locally by endothelial, neurogenic and myogenic activity in the vessel wall and respiratory and cardiac rhythm, frequency domain analysis may provide more detailed information of potential systemic variations within the different groups.

Frequency domain

All 10 min baseline BF signal segments recorded for the 50 individuals exhibited multiple oscillatory components as shown in Figure 2. While individual PSD show no obvious patterns associated with each group, their mean spectra show some discernible peaks within each frequency band and differences in their distribution. Compared with the DM0 group, mean power in respiratory and myogenic bands is attenuated in the DM1 group while mean cardiac power is increased. The CB group exhibit attenuated power in all the low frequency bands compared to both DM0 and DM1, and similar respiratory band power as DM1. Greater power is present in the cardiac band in the CB group than both DM0 and DM1. Absolute oscillatory power over the five bands is shown in Figure 3. There was no significant difference in the absolute total power between any of the groups.

The normalized relative PSD contributions (0-1) of the five frequency bands to the BF signal are shown in Figure 4. No significant differences were found between groups with and without T2DM where the majority of power lies in the low frequency (LF) endothelial, neurogenic and myogenic bands. With calcium channel blocker use, the relative PSD contribution of the high frequency (HF) cardiac band increased significantly over DM0 (p = 0.00017) and DM1 (p = 0.0003). Similarly, in the myogenic band power decreased significantly over DM0 (p = 0.015) and DM1 (p = 0.0006). Neurogenic power also decreased compared with DM0 (p = 0.051) and DM1 (p = 0.073). The decrease in myogenic and increase in the cardiac band contribution to overall power in the CB group seen in Figure 4 is consistent with the higher RF modulated by the calcium channel blocker through a reduction in vascular tone as observed in Table 2.

Examining the relative contributions (0-1) of the components of the three LF bands of the BF signal (see Table 3) shows no significant difference between the powers in these bands between the groups. The large reduction in neurogenic and myogenic activity combined with increased cardiac power attributable to the calcium channel blocker[35] (shown in Figure 4) is reflected in the increased contribution to the LF of the endothelial band. While the frequency domain analysis reveals more

information around the mechanisms influencing the BF signal, it still does not provide a reliable method to discriminate between the groups.

Complexity:

LZC was estimated for baseline BF in all participants and showed relative consistency over the 15 x 40 second epochs in all groups, Figure 5. The BF signal appeared less variable and has fewer unique states (a lower LZC) in the DM1 group than the DM0 group and this was more pronounced with the CB group. However, there is little difference in complexity in the absence or presence of T2DM alone. The BF LZC-index (mean value over the 15 epochs for each individual), Figure 6, fell from 0.362 ± 0.03 in the absence of T2DM to 0.344 ± 0.05 with T2DM. The LZC with calcium channel blocker use was 0.302 ± 0.05. The BF LZC-index was found to correlate positively with dilator capacity ($r = 0.47$, $p = 0.001$) and relative power in the respiratory band ($r = 0.52$, $p = 0.0001$) and negatively with RF ($r = -0.37$, $p = 0.008$) and relative power in the cardiac band ($r = -0.56$, $p = 0.00004$). The LZC-index was found to be negatively correlated with BMI ($r=-0.31$, $p=0.028$) and CVD risk ($r = -0.32$, $p=0.024$) across all n=50 participants.

The multiscale LZC was computed for all participants over 24 scales corresponding to BF signal sampling rates of 40Hz at scale $\tau = 1$ to 1.67Hz at scale $\tau = 24$ as shown in Figure 7. As the scale length is increased the LZC is also seen to increase, with better separation between the groups at certain scales. LZC was negatively correlated with age in scales $\tau = 2 – 15$ ($r = [-0.28, -0.31]$, $p < 0.05$), BMI in scales $\tau = 14, 15, 20, 21$ ($r = [-0.28, -0.31]$, $p < 0.05$) and CVD risk in scales $\tau = 1 – 12, 14, 15$ ($r = ([-0.27, -0.33]$, $p < 0.05$) across all n=50 participants. The largest difference between the complexity values of the multiscale analysis between the DM0 and DM1 groups is obtained for time scale 15. There is also a higher separation between the DM0 and CB groups at around scale 15 while the greatest separation between the DM1 and CB groups occurs at around scale 10.

To understand how the spectral components of the BF signal influence its information content and hence complexity, we examined the Spearman's correlations between the power bands of the BF signal and MLZC. Figure 8 shows the association of the spectral bands to MLZC complexity at each scale for all three groups combined. Cardiac activity negatively correlated with LZC at all scales except $\tau = 24$ (1.6 Hz sample rate) with the strength of correlation generally increasing until around scale $\tau = 16$ (2.5 Hz sample rate) before sharply reducing. Power in the respiratory band positively correlated with LZC up to scale $\tau = 21$ (1.9 Hz sample rate) reducing rapidly after scale $\tau = 18$ (2.22 Hz sample rate) becoming negative at scale $\tau = 24$. In the LF band, power in the myogenic activity

positively correlated with LZC at scales $\tau \geq 19$ (<2.1 Hz sample rate) and in scales $\tau = 15 – 20$ (2.0 – 2.7 Hz sample rate) in the endothelial range. No significant association was found with power in the neurogenic activity band and MLZC at any scale.

Finally, the LZC and MLZC were tested as features against which to discriminate the different groups. Table 4 shows linear discriminant analysis with leave-one-out cross-validation applied for the LZC (left table) across 15 features (epochs) and MLZC (right table) across 24 features (scales). The LDA classifier was able to classify 30 out of 42 DM0 and DM1 subjects correctly with the LZC, giving 71.4% separability, while with MLZC complexity the classification accuracy between these groups was 83.3%. The highest classification accuracy was achieved when comparing DM0 and CB giving 77.8% separability for LZC values and 86.1% for MLZC complexity values. The lowest separability was achieved between DM1 and CB yielding a 63.6% classification accuracy using the LZC and 68.2% using the MLZC values.

4. Discussion

We set out to investigate whether complexity-based methods could be used to analyze skin BF measurements to discriminate between different groups of individuals at increased risk of or with CVD. The microvascular BF characteristics measured at rest and during a vasoreactivity test were evaluated and shown to be a poor discriminator between the three groups. The low frequency oscillatory rhythms of the recorded microvascular blood perfusion were then assessed in terms of their spectral power. While there was no significant difference in the total power in the BF signals from the three groups we were able to discriminate between the groups with and without calcium channel blocker uptake in the spectral power contained in the myogenic and cardiac frequency bands. Examining the information content of the BF signal revealed a clear and significant different in LZC between the groups with and without calcium channel blockers and that this becomes more pronounced at certain time scales (or sampling rates). Furthermore, by examining the association of the individual spectral bands with the different time scales in MLZC, our findings provide strong evidence that in human skin, the influence of these modulators on information content in the BF signal is strongly affected by the time scale. The results further show that multiscale analysis has strong potential for discriminating between these different groups.

Network perfusion in the time domain

In a recent study, Frisbee et al[2] observe ''the results from the present study suggest that "blood flow" may not be a particularly informative marker of peripheral vascular disease (PVD) risk and outcomes of PVD below a certain easily determined threshold.'' In the current study, the resting BF

is not significantly different between the groups with and without T2DM and consistent with that reported in recent studies[36,37]. As anticipated, the use of calcium channel antagonists for the treatment of hypertension and persisting microcirculatory disorders resulted in a significant increase in resting BF[38] in the CB group over the DM0. The dilatory response to PORH (~5 fold change) in DM0 and DM1 groups was similar to that we have reported previously in healthy forearm skin[32]. In the CB group this was significantly attenuated which is perhaps unsurprising as the microvascular network is already somewhat dilated. So, while there are differences in the time domain metrics of the microvascular network perfusion between the groups, there is little information that can be directly employed, and on its own, is unable to discriminate between them or reliably classify individual signal measurements.

Power-frequency profiles of network perfusion

Microvascular perfusion as measured by LDF is generally accepted as being characterized by the main dynamic modes that lie within five frequency bands contained in the ~0.0095 - ~1.6 Hz range, as described previously[16]. Many studies have considered the frequency domain analysis of LDF signals and employed a variety of techniques. Here we have used Welch's method to estimate the power in the LDF signal at the different frequencies, taken to reflect the activity of the local vaso-control mechanisms and the haemodynamic effects of the heart beat and respiratory activity on the microcirculation. Additionally, the absolute total power in the LDF signal over the frequency range of interest has been calculated to find the relative contribution of a frequency band and its impact on the overall flow motion. LDF analysis in the frequency domain has also been extensively reported using generalized wavelet analysis[16] and empirical mode decomposition[39]. The choice of frequency domain analysis techniques has been discussed previously elsewhere, e.g.[40], involving the consideration of the compromise between time and frequency resolution. As we were investigating the contribution of power in the signal frequency bands and had sufficiently long recordings to estimate that of the lowest frequency band (endothelial, 0.0095 – 0.02 Hz), the fast Fourier transform-based approach provided a direct measure.

Our study has shown that there was no significant difference in the absolute total power between the three groups. The power-frequency profiles for each individual were unique although variation could be seen in the spectra when comparing the means. Examining the relative PSD contributions of the five frequency bands, the majority of the power arose from the three LF bands similar to that reported in studies of both healthy[32] and individuals with disease[41,42]. With calcium channel blocker use, the distribution of the relative power over the five frequency bands changed significantly. The

majority of the power in the LDF signal lay in the heart beat rather than the LF bands indicating higher pulse wave transmission[43]. Myogenic and neurogenic contributions were suppressed as was that in the respiratory band. Examining the relative power in the LF bands alone revealed that this overall decrease was reflected in an uploading in the endothelial contribution while the myogenic band decreased as anticipated with calcium channel blocker use. With T2DM, the endothelial band LF contribution decreased, although not significantly. Thus, examining the contribution to the BF from the main five modulating processes and considering the relative balance between them reveals more functional information regarding the characteristics on individual BF signals. However, this is insufficient to reliably distinguish between the groups here or provide definitive and consistent interpretation of microvascular function[10].

Complexity of network perfusion

It has recently been suggested that an increased capacity for variability in blood flux is indicative of a more effective microvascular system[6,9,42] with a lower variability in microvascular activity corresponding to a loss of the system's ability to adapt under pathophysiological conditions. From a signal perspective, variability in BF arises from the cumulative activity of all the process modulating BF and their temporal variation. Frequency domain analysis has been used to estimate the contribution of these processes to the LDF signal but cannot track the variability or reactivity of the signal over short time scales. Algorithmic complexity of the time series data yields a measure of the variability or predictability of the time series and can therefore be used to assess signals at short time scales. In general, LZC is determined from a transformation of the original time series to a binary sequence through comparison with a threshold such as the median or mean value[20] although dividing the sequence into epochs could, of course, yield different threshold for each epoch. This approach can also be associated with loss of essential information such as the dynamics or trajectory of the signal[44] and we have used a delta encoding here to localize the signal change at each time point rather than to a fixed reference point. To prevent over-estimating the complexity measure we have used the exhaustive method which gives us the lower bound of the signal variability.

Using this approach, we have shown that the information content of the BF signal was lower in the DM1 group than the DM0 one, albeit without statistical significance, while the CB group was significantly less complex. For all groups, over time (epochs) the complexity of the BF signal changed dynamically and, as it is not possible to synchronize groups to any of the modulating process of the microvascular perfusion, variation in SEM occur over epochs. This variation of complexity is consistent with that of Tigno et al[7] in the skin of primates although they found that there was larger

separation at some epochs than the data presented here obtained in humans. The LZC-index, aggregating the variation in epochs, showed a significant difference in the information content when a calcium channel blocker was taken. The spectral analysis showed the uprating of the cardiac power, a relatively high frequency and periodic modulator of BF, and a downrating in other lower frequency bands. Consequently, the BF signal had proportionally more periodic content at higher power levels and the complexity was reduced as the information content was lower. A reduction of spontaneous variation in flowmotion activity in vascular beds at risk of CVD and metabolic disease[6] may contribute to attenuated network flexibility and adaptation in the presence of physiological and pathological challenge. The improvement in baseline blood flux with calcium channel antagonist was as expected but also showed a very limited dilator response and significant reduction in temporal variation in all complexity measures consistent with observations in animal models[9]. In the data presented here, increased BMI and increased CVD risk reduced BF temporal variability.

In previous work by Kalev et al[45], it was found that traditional LZC was unable to account for the high frequency components in some signals and was only 50% accurate in dichotomizing states from EEG signals. Using MLZC this increased to 86% by accounting for the different frequencies of information content. We have previously applied MLZC to BF and oxygenation signals recorded in forearm skin clamped at 33°C and during local thermal hyperaemia at 43°C and found that classification accuracy between these two haemodynamic states of up to 90% could be achieved. Thus, we calculated the LZC for each individual over 24 scales corresponding to sample rates reducing from 40 Hz to 1.67 Hz. As the sampling rate decreases with increasing scale, the complexity increases until it reaches or passes the Nyquist frequency of the original time series. If the maximum frequency of interest is governed by an upper limit of heart rate of 1.6 Hz the Nyquist frequency will be twice this or 3.2 Hz which corresponds to scale $\tau = 12$. Above the scale corresponding to the heart rate of the individual time series, the relatively periodic oscillatory influence will be diminished and the signal contain more information. To reach higher scales, longer recordings are required and we have shown[22] that there is a lower limit on the number of samples required to achieve repeatable and accurate complexity analysis limiting the lowest frequency cut off. We observed different scales at which the maximum separation between groups occurred with DM0-DM1 and DM0-CB at scale $\tau = 15$ and DM1-CB at $\tau = 10$. Similar behavior was shown by Humeau et al[46] in a recent study when BF signals were filtered for frequencies associated with heart rate (~0.6 – 2 Hz) using a multiscale entropy analysis. Age, BMI and CVD risk were all associated with a reduction in complexity, or signal variability, at certain scales, the only common one being $\tau = 15$.

The MLZC measures the information content of the BF signal at different time scales, or sampling frequencies, but the power-frequency profile of the signal remains constant. To understand the influence of the modulation of the BF signal by the different frequency bands they were correlated with the complexity measure at each scale. Heart beat and respiration had significant large but opposite correlations with complexity until the longest scale. It is known that skin sympathetic nerve activity is modulated by respiration and that the firing of cutaneous vasoconstrictor neurones is temporally coupled to both cardiac and respiratory oscillations[47]. Heart rate variability is also known to contribute to complexity of the BF signal[48,49] and cardiac rhythm is modulated by respiratory oscillation[50]. This coupling of the two HF components offers a possible partial explanation as to why the MLZC increases with scale. Both heart rate and respiration are relatively periodic with little spontaneous variability under measurement conditions so their conjugate influence diminishes as the sampling frequency is decreased. Thus, at longer time scales, where the resampled BF signal covers a longer time period, the lower frequencies associated with flowmotion (that generally contain most of the power in the signal) contribute more to signal variability. This results in greater complexity. At the higher scales this LF influence becomes significant in both the endothelial and myogenic bands which have higher correlation with complexity above the Nyquist frequency.

Linear discriminant analysis classifiers are good for dimensionality reduction, they are simple in terms of implementation and can be very quickly trained. The LDA technique has been widely used from optical character and facial recognition[25,26,51,52] to clinical applications[11,45,53] and thus have been shown to be a very promising tool for discriminating different pathophysiological groups. Here, the LDA classifier was examined in order to separate the groups DM0-DM1-CB based on the complexity analysis in 15 epochs and the multiscale complexity in 24 scales. The LDA using the 24 features of the MLZC exhibits better performance overall. However, it was significantly better for the groups DM0 and CB with a classification accuracy 86.1%. The relativel low n for the DM1 and CB groups may explain the apparent discordance between Figure 7 and Table 4 but also the value of the LDA. The mean MLZC of DM0 and DM1 are close over all scales but by employing the scale LZCs as features the LDA can distinguish between 83%. On the other hand, the small numbers in the CB and DM1 groups appear well separated by the group means over all scales but the variation in the groups makes these features less reliable achieving only 68% accuracy. Higher numbers in these groups are likely to improve accuracy. Nevertheless, by this test we showed that the characteristics of the multiscale analysis can be used in classification algorithms to separate between different data sets derived from groups with unique features.

5. Conclusions

Robust and consistent description of the dynamics within the microcirculation cannot be achieved with time and frequency domain methods alone in either resting states or during the application of a standard stressor. The combination of time, frequency and complexity analysis yields deeper understanding of the loss of system flexibility which may prevent the microvascular networks from adapting to an imposed stressor and some of the parameters that influence this. Attenuation of flowmotion patterns increases with CVD risk factors and temporal behavior and adaptivity further declines with prophylactic treatment. We have shown that complexity-based methods applied to signals derived from the skin microvasculature can discriminate between groups of individuals at increasing risk of developing CVD. The observed association between dilator capacity and a reduced complexity of the BF signal estimated using the Lempel-Ziv complexity algorithm suggest that a decline in spatial heterogeneity of network perfusion derived from the activity of local endothelial, myogenic and neurogenic vaso-mechanisms limits the adaptive capability of the microvasculature. Use of calcium channel blockers for the treatment of hypertension and persisting microcirculatory disorders, was associated with a further decline in the variability of the BF signal which had a LZC (fewer unique states). Our findings suggest that the significant attenuation of the network's flexibility and adaptability with increasing CVD risk make these methods a promising approach for further analysis of microvascular function. Nonlinear measures offer promise in discriminating more effectively between these different mechanistic influences on network functionality and flexibility and now need to be extended to cohorts under further pathological conditions.

Limitations

Our study reveals novel understanding of the relationship between time, frequency and complexity analysis of time series derived from the microvasculature in the presence of increasing risk of CVD but may also be subject to some limitations. The calcium channel blocker group contained people with and without T2DM and was of small size, n=8. The T2DM group were being treated which will have impacted upon the recorded blood flux measurements. Nevertheless, we have shown that differences could be detected between these groups through a systematic analysis of the recorded time series. The power-frequency profiles do not have a dominant frequency of oscillation in the defined low frequency bands in contrast to the clear peaks around 1 Hz in the cardiac band, consistent with a resting heart rate of ~60 beats per minute. The range and border of the frequency bands used have previously been defined by others[16] and it is possible that the LF profiles comprise multiple frequency components that may vary with time. The FFT, unlike the wavelet transform,

cannot easily be time-localized so we were unable to explore this here. It is reasonable to assume from the data presented here that the range and limits of the frequency bands will differ between individuals and pathophysiological conditions.

Perspective

The time, frequency and complexity domain analysis of microvascular blood flow can provide robust parameters that provide a better understanding of the relationship between microvascular perfusion and CVD risk and account, to some degree, for the temporal scale of their origin in terms of the local and systemic physiological activity. We have shown that the synchronicity of rhythms in the modulators of skin blood flux contributes to the complexity of microvascular blood flow and that this reduces with CVD risk as flow becomes more homogenous and predictable. These multiple domain analyses and findings provide a platform from which to investigate microvascular impairment in the skin.

Acknowledgements

The WELCOME[12] trial was supported by the National Institute of Health Research (NIHR) through the NIHR Southampton Biomedical Research Centre. Marjola Thanaj was supported by a UK EPSRC DTP PhD studentship. CDB and ES were supported in part by the NIHR Southampton Biomedical Research Centre.

Figure Legends

Figure 1: Examples of blood flux signals recorded from skin at the forearm at ambient room temperature in (A) individual without type 2 diabetes mellitus, (B) individual with type 2 diabetes mellitus and (C) an individual at rest and during the response to arterial occlusion (180 mmHg for 3 minutes).

Figure 2: Individual (dotted) and mean (solid) PSD spectra for the three test groups DMO n=28 black, DM1 n=14 red, CB n=8 green.

Figure 3: Absolute total power in baseline BF signal measured in forearm skin. Data are presented as median and IQR for n=28, n=14, n=8.

Figure 4: PSD contributions to baseline BF signal across five frequency bands recorded at the forearm. Data are presented as median and IQR for n=28, n=14, n=8. * $p < 0.05$, ** $p < 0.001$.

Figure 5: LZC of BF for the three test groups. Data are mean ± SEM for n=28, n=14, n=8.

Figure 6: Comparison of LZC-index expressed as mean across the 15 epochs between test groups. Data are mean ± SD for n=28, n=14, n=8.

Figure 7: MLZC of baseline BF signal measured in forearm skin. Data are presented as median and IQR for n=28, n=14, n=8.

Figure 8: Correlation of spectral bands with MLZC for baseline BF signal measured in forearm skin for n= 50.

Figure 1

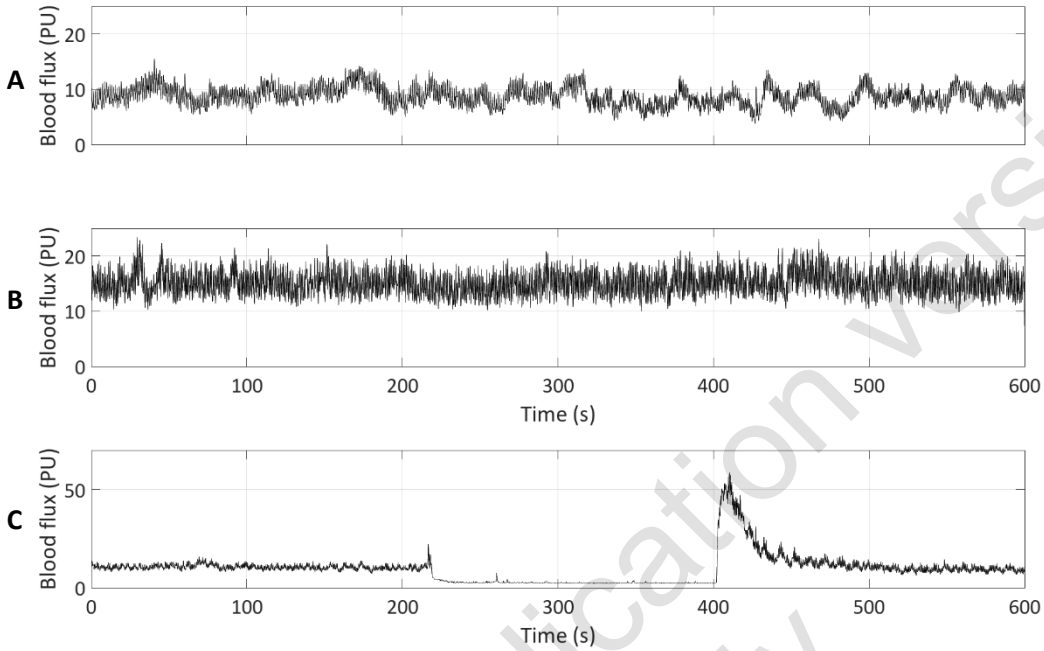

Figure 2

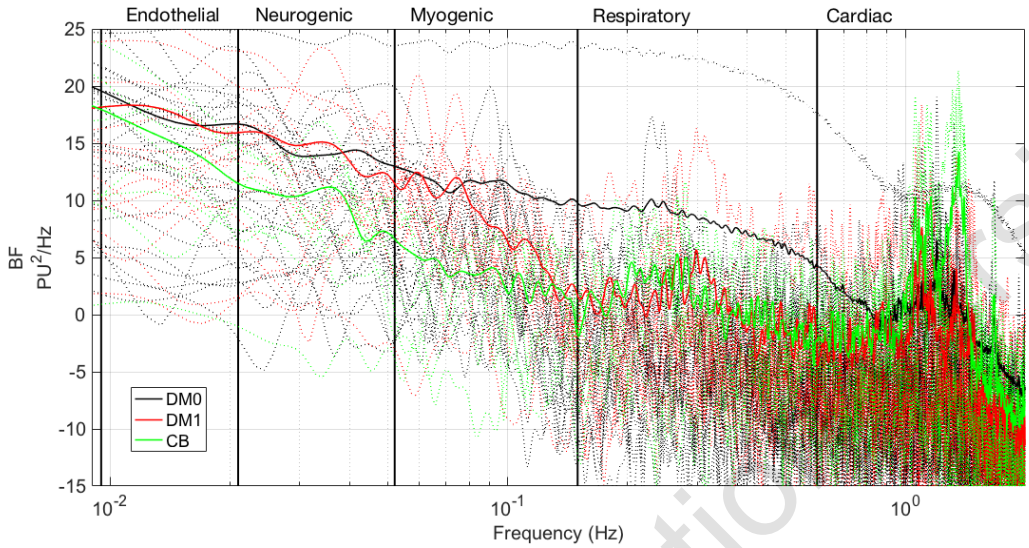

Figure 3

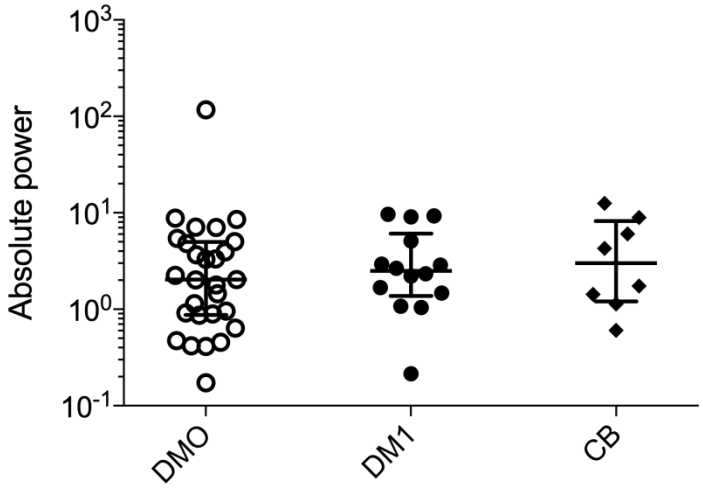

Figure 4

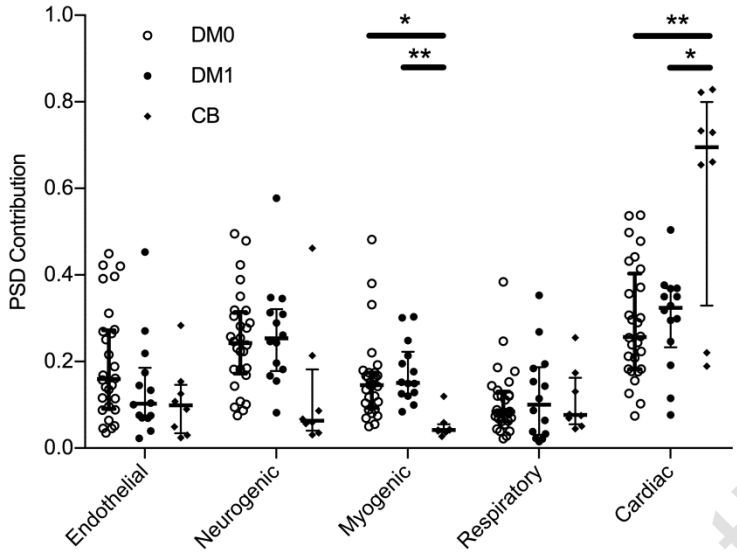

Figure 5

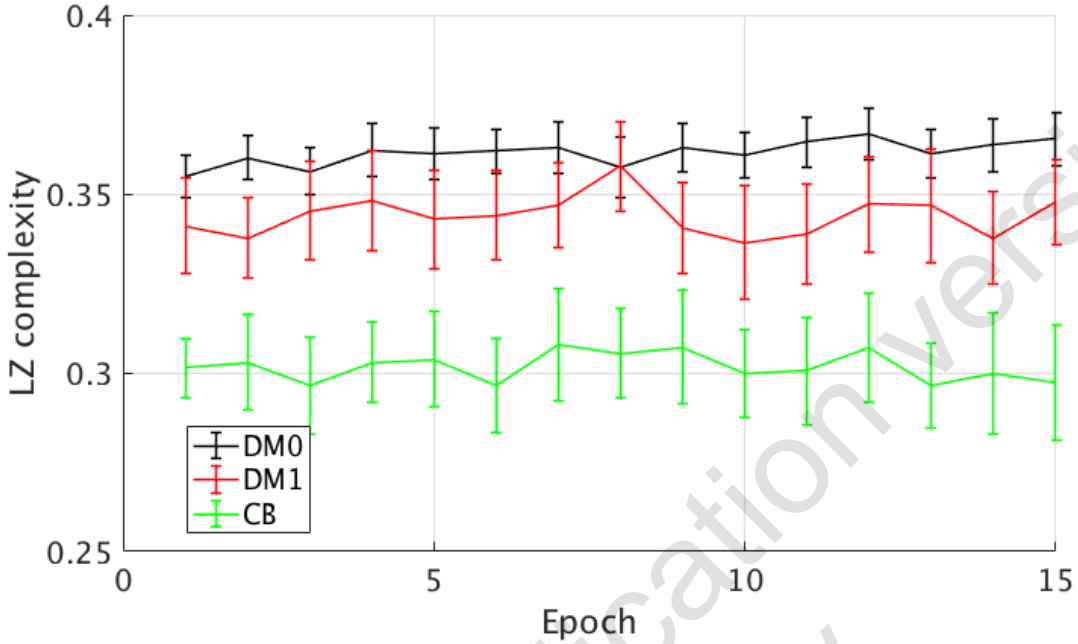

Figure 6

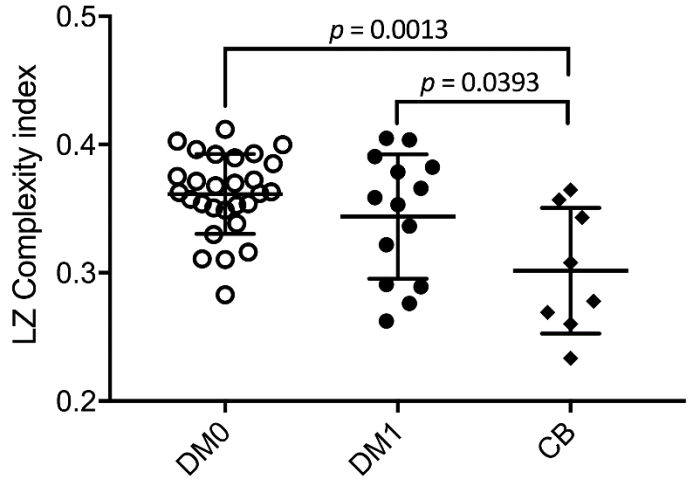

Figure 7

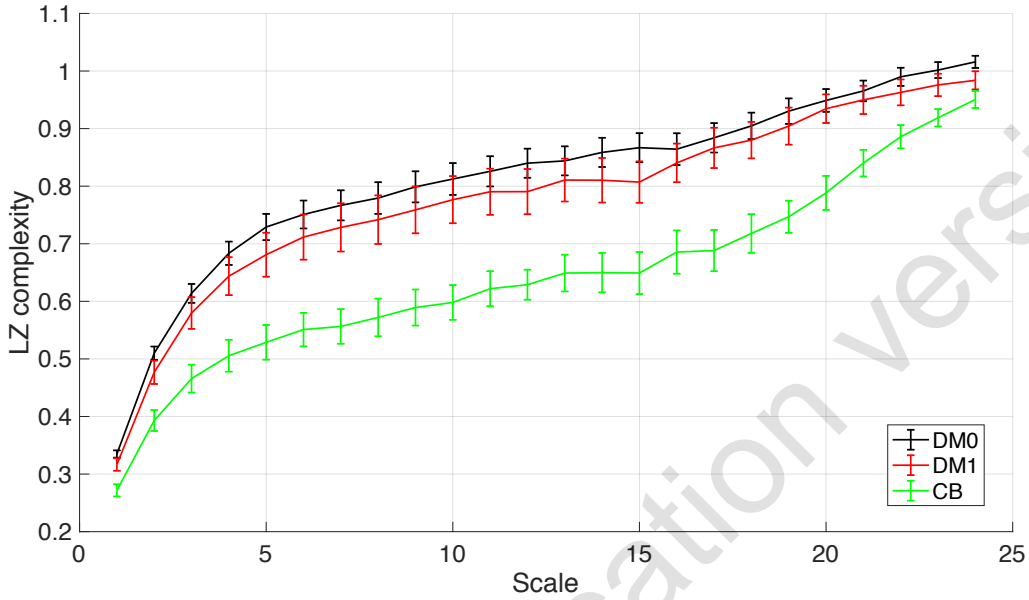

Figure 8

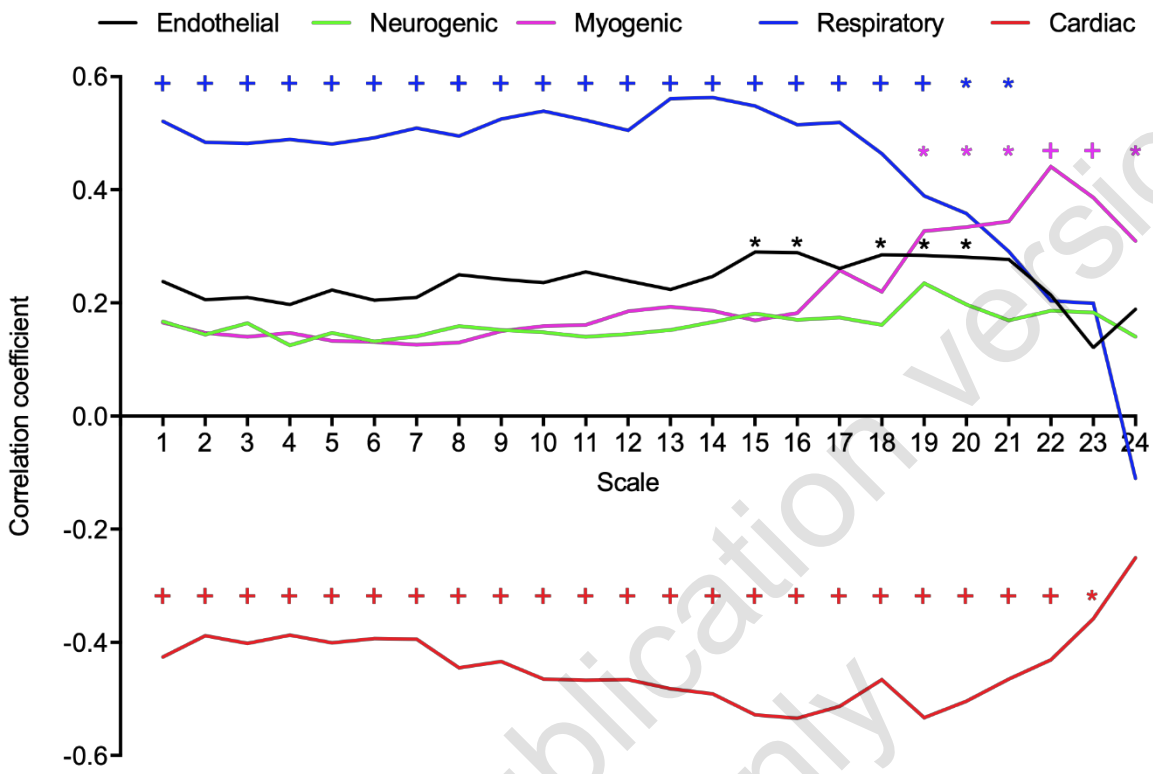

Tables

Table 1: Characteristics and composition of test groups. Data are mean ± SD.

Table 2: Measured BF parameters. Data are mean ± SD for n=28, n=14, n=8.

Table 3: PSD contributions in BF signal in the three LF frequency bands. Data are mean and SD for n=28, n=14, n=8.

Table 4: Confusion matrices of the LDA classifier in BF signal for the three test groups.

Table 1: Characteristics and composition of test groups.

	DM0	DM1	CB
Age (years)	52.1 ± 6.3	51.4 ± 8.2	56.8 ± 5.2
Sex	15M/13F	11M/3F	4M/4F
BMI (kg/m^2)	31.2 ± 4.3	30.6 ± 1.9	37.2 ± 3.0
CVD Risk (%)	9.9 ± 6.4	17.4 ± 9.0	17.4 ± 7.1
Systolic BP (mmHg)	139 ± 16.0	134 ± 16.0	130 ± 13.4
Diastolic BP (mmHg)	85 ± 11.4	84 ± 8.0	91 ± 9.5
Diabetes duration (years)	-	4.8 ± 7.5	-
METS (kcal/kg/h)	1.24 ± 0.20	1.29 ± 0.26	1.16 ± 0.14
HOMA-IR	2.6 ± 1.4	4.5 ± 3.2	4.1 ± 2.6
HbA1c (mmol/l)	5.8 ± 0.4	7.3 ± 1.1	6.2 ± 0.5

Subjects were stratified by the absence (DM0) or presence (DM1) of T2DM, and use of calcium channel blocker medication (CB) with and without T2DM (n=5 with T2DM). Data are mean ± SD.

Table 2: Measured BF parameters. Data are mean ± SD for n=28, n=14, n=8.

	DM0	DM1	CB
Resting BF RF (PU)	10.7 ± 4.3	13.1 ± 5.3	17.2 ± 10.7*
Maximum BF MF (PU)	51.3 ± 24.5	64.7 ± 22.5	50.7 ± 21.6
Dilator capacity MF/RF (fold change)	5.0 ± 1.7	5.4 ± 1.8	3.2 ± 1.1*+

* significant difference from DMO, $p < 0.05$; + significant difference from DM1, $p < 0.05$

Table 3: PSD contributions in BF signal in the three LF frequency bands. Data are mean ± SD for n=28, n=14, n=8.

Group	Endothelial	Neurogenic	Myogenic
DM0	0.31 ± 0.17	0.40 ± 0.12	0.29 ± 0.18
DM1	0.23 ± 0.13	0.45 ± 0.10	0.32 ± 0.13
CB	0.39 ± 0.15	0.38 ± 0.12	0.23 ± 0.12

Table 4: Confusion matrices of the LDA classifier in BF signal for the three test groups.

LZC			
	DM0	**DM1**	**Class. accuracy**
DM0	24	8	**71.4%**
DM1	4	6	
	DM0	**CB**	**77.8%**
DM0	25	5	
CB	3	3	
	DM1	**CB**	**63.6%**
DM1	10	4	
CB	4	4	

MLZC			
	DM0	**DM1**	**Class. accuracy**
DM0	24	3	**83.3%**
DM1	4	11	
	DM0	**CB**	**86.1%**
DM0	26	3	
CB	2	5	
	DM1	**CB**	**68.2%**
DM1	10	3	
CB	4	5	

References

1. Segal SS. Regulation of blood flow in the microcirculation. *Microcirculation*. 2005;12:33–45.

2. Frisbee JC, Butcher JT, Frisbee SJ, Olfert, IM, Chantler, PD, Talbone, LE, d'Audiffret AC, Shrader CD, Goodwill AG, Stapleton PA, Brooks SD, Brock RW, Lombard JH. Increased peripheral vascular disease risk progressively constrains perfusion adaptability in the skeletal muscle microcirculation. *Am J Physiol Heart Circ Physiol*. 2016;310:488–504.

3. Lemaster K, Jackson D, Goldman D, Frisbee JC. Insidious incrementalism: the silent failure of the microcirculation with increasing peripheral vascular disease risk. *Microcirculation*. 2017;24:e12332.

4. Roustit M, Cracowski JL. Non-invasive assessment of skin microvascular function in humans: an insight into methods. *Microcirculation*. 2012;19-47-64.

5. Kvernmo HD, Stefanovska A, Kirkebøen KA, Kvernebo K. Oscillations in the human cutaneous blood perfusion signal modified by endothelium-dependent and endothelium-independent vasodilators. *Microvasc Res*. 1999;57:298–309.

6. Clough GF, Kuliga KZ, Chipperfield AJ. Flow motion dynamics of microvascular blood flow and oxygenation: Evidence of adaptive changes in obesity and type 2 diabetes mellitus/insulin resistance. *Microcirculation*. 2017;24:e12331.

7. Tigno XT, Hansen BC, Nawang S, Shamekh R, Albano AM. Vasomotion becomes less random as diabetes progresses in monkeys. *Microcirculation*. 2011;18:429–39.

8. Gryglewska B, Necki M, Zelawki M, Cwynar M, Baron T, Mrozek M, Grodzicki T. Fractal dimensions of skin microcirculation flow in subjects with familial predisposition or newly diagnosed hypertension. *Cardiol J*. 2011;18:26–32.

9. Frisbee JC, Goodwill AG, Frisbee SJ, Butcher TJ, Wu F, Chantler PD. Microvascular perfusion heterogeneity contributes to peripheral vascular disease in metabolic syndrome: metabolic syndrome and microvascular perfusion. *J Physiol*. 2016;594:2233–2243.

10. Kuliga KZ, Gush, Clough GF, Chipperfield AJ. Time-dependent behavior of microvascular blood flow and oxygenation: a predictor of functional outcomes. *IEEE Trans Biomed Eng*. 2018;65:1049–1056.

11. Thanaj M, Chipperfield AJ, Clough GF. Multiscale analysis of microvascular blood flow and oxygenation. *IFMBE Proc*. 2019;68/2:195–200.

12. Scorletti E, Bhatia L, McCormick KG, Clough GF, Nash K, Calder PC, Byrne CD. Design and rationale of the WELCOME trial: A randomised, placebo controlled study to test the efficacy of purified long chain omega-3 fatty treatment in non-alcoholic fatty liver disease. *Contemporary Clinical Trials*. 2014:37;301–311.

13. Kuliga KZ, McDonald EF, Gush R, Michel C, Chipperfield AJ, Clough GF. Dynamics of microvascular blood flow and oxygenation measured simultaneously in human skin. *Microcirculation*. 2014;21:562–573.

14. Roustit M, Maggi F, Isnard S, Hellmann M, Bakken B, Cracowski JL. Reproducibility of a local cooling test to assess microvascular function in human skin. *Microvasc Res*. 2010;79:34–39.

15. Svalestad J, Hellem S, Vaagbø G, Irgens Å, Thorsen E. Reproducibility of transcutaneous oximetry and laser Doppler flowmetry in facial skin and gingival tissue. *Microvasc Res*. 2010;79:29–33.

16. Stefanovska A, Bracic M, Kvernmo HD. Wavelet analysis of oscillations in the peripheral blood circulation measured by laser Doppler technique. *IEEE Trans Biomed Eng*. 1999:46;1230–1239.

17. Lempel A, Ziv J. On the complexity of finite sequences. *IEEE Trans Information Theory*. 1976;22:75–81.

18. Liu L, Miao S. The complexity of binary sequences using logistic chaotic maps. *Complexity*. 2016;21:121–129.

19. Zhang XS, Zhu YS, Thakor NV, Wang ZZ. Detecting ventricular tachycardia and fibrillation by complexity measure. *IEEE Trans Biomed Eng*. 1999;46:548–555.

20. Aboy M, Hornero R, Abasolo D, Alvarez D. Interpretation of the Lempel-Ziv complexity measure in the context of biomedical signal analysis. *IEEE Trans Biomed Eng*. 2006;53:2282–2288.

21. Albano AM, Brodfuehrer PD, Cellucci CJ, Tigno XT, Rapp PE. Time series analysis, or the quest for quantitative measures of time dependent behavior. *Philippine Science Letters*. 20018;1:18-31.

22. Thanaj M, Chipperfield AJ, Clough GF, Analysis of microvascular blood flow and oxygenation: Discrimination between two haemodynamic steady states using nonlinear measures and multiscale analysis. *Comput Biol Med*. 2018;102:157–167.

23. Yang ACC, Hseu SS, Yien HW, Goldberger AL, Peng CK. Linguistic analysis of the human heartbeat using frequency and rank order statistics. *Phys Rev Lett*. 2003;90:108103.

24. Costa M, Goldberger AL, Peng CK. Multiscale entropy analysis of complex physiologic time series. *Phys Rev Lett*. 2002;92:068102.

25. Jian Y, Frangi AF, Jing-Yu Y, David Z, Zhong J. KPCA plus LDA: a complete kernel Fisher discriminant framework for feature extraction and recognition. *IEEE TPAMI*. 2005;27:230-244.

26. Mika S, Ratsch G, Weston J, Scholkopf B, Smola A, Muller K. Constructing descriptive and discriminative nonlinear features: Rayleigh coefficients in kernel feature spaces. *IEEE TPAMI*. 2003;25:623-628.

27. Wallace TM, Levy JC, Matthews DR. Use and abuse of HOMA modeling. *Diabetes Care*. 2004;27: 1487–1495.

28. Hills AP, Mokhtar N, Byrne NM. Assessment of physical activity and energy expenditure: an overview of objective measures. *Front Nutr*. 2014;1:5.

29. Hippisley-Cox J, Coupland C, Vinogradova Y, Robson J, Minhas, R, Sheikh A, Brindle P. Predicting cardiovascular risk in England and Wales: prospective derivation and validation of QRISK2. *BMJ*. 2008;336:1475–1482.

30. Zegarra-Parodi R, Snider EJ, Park PY, Degenhardt BF. Laser Doppler flowmetry in manual medicine research. *J Am Osteopath Assoc*. 2014;114:908-917.

31. Yvonne-Tee GB, Rasool AH, Halim AS, Rahman ARA. Reproducibility of different laser Doppler fluximetry parameters of postocclusive reactive hyperemia in human forearm skin. *J Pharmacol Toxicol Methods*. 2005;52:286–292.

32. Clough GF, Chipperfield AJ, Byrne CD, de Mul F, Gush R. Evaluation of a new high power, wide separation laser Doppler probe: potential measurement of deeper tissue blood flow. *Microvasc Res*. 2009;78:155–61.

33. Wahlberg E, Fagrell B. Spatial and temporal variation in laser Doppler flux values in healthy lower limbs: comparison between the standard and the multiprobe. *Int J Microcirc Clin Exp*. 1994;14: 343–346.

34. Roustit M, Cracowski JL. Assessment of endothelial and neurovascular function in human skin microcirculation. *Trends Pharmacol Sci*. 2013; 34:373–384.

35. Palma-Gámiz JL. High blood pressure and calcium antagonism. *Cardiology*. 1997;88:39-46.

36. Papadogeorgos NO, Jörneskog G, Bengtsson M, Kahan T, Kalani M. Severely impaired microvascular reactivity in diabetic patients with an acute coronary syndrome. *Cardiovasc Diabetol*. 2016;15:66,

37. Hsiu H, Hu HF, Tsai HC. Differences in laser-Doppler indices between skin-surface measurement sites in subjects with diabetes. *Microvasc Res*. 2018;115:1–7.

38. Li XF, Wang YP. Laser Doppler flowmetry for assessment of myocardial microperfusion in the beating rat heart. *Vasc Pharmacol*. 2007;46:207–214.

39. Humeau-Heurtier A, Klonizakis M. Processing of laser Doppler flowmetry signals from healthy subjects and patients with varicose veins: Information categorisation approach based on intrinsic mode functions and entropy computation. *Med Eng Phys*. 2015;37:553–559.

40. Rossi M, Carpi A, Di Maria C, Galetta F, Santoro G. Spectral analysis of laser Doppler skin blood flow oscillations in human essential arterial hypertension. *Microvasc Res*. 2006;72:34–41.

41. Newman JMB, Dwyer RM, St-Pierre P, Richards SM, Clark MG, Rattigan S. Decreased microvascular vasomotion and myogenic response in rat skeletal muscle in association with acute insulin resistance. *J Physiol*. 2009;587: 2579–2588.

42. Gryglewska B, Necki M, Cwynar M, Baron T, Grodzicki T. Neurogenic and myogenic resting skin blood flowmotion in subjects with masked hypertension. *J Hypertens*. 2010;28:551-558.

43. Pozzobon CR, Gismondi RAOC, Bedirian R, Ladeira MC, Neves MF, Oigman W. Functional vascular study in hypertensive subjects with type 2 diabetes using Losartan or Amlodipine. *Arq Bras Cardiol*. 2014;103:51-59.

44. Butcher JT, Goodwill AG, Stanley SC, Frisbee JC. Blunted temporal activity of microvascular perfusion heterogeneity in metabolic syndrome: a new attractor for peripheral vascular disease? *Am J Physiol Heart Circ Physiol*. 2013;304:H547–H558.

45. Kalev K, Bachmann M, Orgo L, Lass J, Hinrikus H. Lempel-Ziv and multiscale Lempel-Ziv complexity in depression. *Proc IEEE EMBC*. 2015;37:4158–4161.

46. Humeau-Heurtier A, Wu CW, Wu SD, Mahe G, Abraham P. Refined multiscale Hilbert–Huang spectral entropy and its application to central and peripheral cardiovascular data. *IEEE Trans Biomed Eng*. 2016;63:2405–2415.

47. Fatouleh R, Macefield VG. Cardiorespiratory coupling of sympathetic outflow in humans: a comparison of respiratory and cardiac modulation of sympathetic nerve activity to skin and muscle. *Exp Physiol*. 2013;98: 1327–1336.

48. Sassi R, Cerutti S, Lombardi F, Malik M, Huikuri HV. Advances in heart rate variability signal analysis: joint position statement by the e-Cardiology ESC Working Group and the European Heart Rhythm Association co-endorsed by the Asia Pacific Heart Rhythm Society. *Europace*. 2015;17:1341–1353.

49. Wang G, Jia S, Li H, Wang Z, Zhang W. Exploring the relationship between blood flux signals and HRV following different thermal stimulations using complexity analysis. *Sci Rep*. 2018;8:8982.

50. Simms AE, Paton JFR, Allen AM, Pickering AE. Is augmented central respiratory–sympathetic coupling involved in the generation of hypertension? *Resp Physiol Neurobiol*. 2010;174:89–97.

51. Belhumeur PN, Hespanha JP, Kriegman DJ. Eigenfaces vs. Fisherfaces: recognition using class specific linear projection. *IEEE Trans Pattern Anal Mach Intell*. 1997;19:711-720.

52. Xilin C, Jie Y, Jing Z, Waibel A. Automatic detection and recognition of signs from natural scenes. *IEEE Trans Image Process*. 2004;13:87-99.

53. Costa M, Healey JA Multiscale entropy analysis of complex heart rate dynamics: discrimination of age and heart failure effects. *Comput Cardiol*. 2003;30:705-708.